Structural Characterization by Tandem Mass Spectrometry of the Posttranslational Polyglycylation of Tubulin

Joëlle Vinh,*,‡ James I. Langridge,§ Marie-Hélène Bré,|| Nicolette Levilliers,|| Virginie Redeker,‡ Denis Loyaux,⊥ and Jean Rossier‡

Ecole Supérieure de Physique et de Chimie Industrielles de la Ville de Paris, Laboratoire de Neurobiologie, CNRS UMR 7637, 10 rue Vauquelin, 75231 Paris Cedex 05, France, MICROMASS UK Ltd., Floats Road Wythenshawe, Manchester M23 9LZ, U.K., University Paris-Sud, Laboratoire de Biologie Cellulaire 4, CNRS URA 2227, 91405 Orsay, France, and SYNTHELABO RECHERCHE, Groupe de Biochimie Structurale, 92500 Rueil Malmaison, France

Received September 24, 1998; Revised Manuscript Received December 11, 1998

ABSTRACT: Polyglycylation is a posttranslational modification specific to tubulin. This modification was originally identified in highly stable microtubules from *Paramecium* cilia. As many as 34 posttranslationally added glycine residues have been located in the C-terminal domains of *Paramecium* α- and *β*-tubulin. In this study, post source decay matrix-assisted laser desorption/ionization mass spectrometry (PSD MALDI MS) and electrospray ionization on a hybrid quadrupole orthogonal time-of-flight tandem mass spectrometer (ESI Q-TOF MS/MS) were both used to demonstrate that a single molecule of *β*-tubulin, from either dynamic cytoplasmic microtubules or stable axonemal microtubules, can be glycylated on each of the last four C-terminal glutamate residues Glu[437], Glu[438], Glu[439], and Glu[441] in the sequence [427]DATA-EEEGEFEEEGEQ[442]. In both dynamic and stable microtubules the most abundant *β*-tubulin isoform contains six posttranslationally added glycine residues: two glycine residues on both Glu[437] and Glu[438] and one glycine residue on both Glu[439] and Glu[441]. The number and relative abundance of glycylated isoforms of *β*-tubulin in both cytoplasmic and axonemal microtubules were compared by MALDI MS.[1] The abundance of the major glycylated isoforms in axonemal tubulin decreases regularly with glycylation levels from 6 to 19 whereas it drops abruptly in cytoplasmic tubulin with glycylation levels from 6 to 9. However, the polyglycine chains are similarly distributed on the four C-terminal glutamate residues of cytoplasmic and axonemal tubulin. The polyglycylation results in bulky C-terminal domains with negatively charged surfaces, all surrounding the microtubular structure.

Tubulin, the major constituent of microtubules, is a heterodimeric protein composed of two 50 kDa subunits, designated α- and *β*-tubulin. Both subunits are encoded by multigene families, and both subunits undergo several posttranslational modifications including acetylation, phosphorylation, C-terminal detyrosination/tyrosination, C-terminal deglutamylation, and polyglutamate and polyglycine side-chains addition (for reviews, see refs 1 and 2). With the exception of acetylation, these modifications are located within the last 15 C-terminal residues of α- and *β*-tubulin. The C-terminal domains are exposed on the surface of microtubules, and it is thought that they are involved in microtubule assembly *(3)*.

Polyglycylation, polyglutamylation, and detyrosination/tyrosination have not been described in proteins other than tubulin. Polyglycylation, the subject of this report, involves the formation of lateral polyglycine chains in which the first glycine residue forms an amide bond with the *γ*-carboxyl group of a glutamate residue in the backbone sequence. This modification was first described in *Paramecium* cilia where 3−34 glycines are added to both α and *β* subunits *(4)*. Subsequently, polyglycylation was described in bull sperm (7−13 glycines added to *β*) *(5)*, in sea urchin sperm (up to 12 glycines added to α and up to 11 added to *β*) *(6)*, and in *Giardia lambia* (2−23 glycines added to α) *(7)*. Immunocytochemical studies have demonstrated the presence of this modification in flagellated and ciliated cells from both protists and metazoans *(8−10)*.

In a previous report regarding the polyglycylation of *Paramecium* tubulin, one glutamate residue in α-tubulin, Glu[445], and one glutamate residue in *β*-tubulin, Glu[437], were shown to be involved in the linkage of polyglycine side chains *(4)*. However, it was not possible to exclude additional sites of modification. The polyglycylated C-terminal peptides of *Paramecium* *β*-tubulin released by proteolysis with endoproteinase Asp-N correspond to the C-terminal sequence [427]DATAEEEGEFEEEGEQ[442], in which the last four glutamate residues may be glycylated: Glu[437], Glu[438], Glu[439], and Glu[441]. A preliminary study demonstrated the feasibility of a complete structural study of polyglycylation by collision-induced dissociation/post source decay matrix-assisted laser desorption ionization time-of-flight (CID/PSD MALDI-TOF)

* To whom correspondence should be sent. Tel: (33) (0) 1-40-79-47-64. Fax (33) (0) 1-40-79-47-57. E-mail: joelle.vinh@espci.fr.
‡ CNRS UMR 7637.
§ MICROMASS UK Ltd.
|| CNRS URA 2227.
⊥ SYNTHELABO RECHERCHE.

[1] Abbreviations: MAPs, microtubule associated proteins; CID, collision-induced dissociation; PSD, post source decay; MALDI, matrix-assisted laser desorption/ionization; TOF, time-of-flight; nanoESI: nano-electrospray ionization; Q-TOF: quadrupole orthogonal acceleration time-of-flight; HPLC, high-performance liquid chromatography; TFA, trifluoroacetic acid; MS, mass spectrometry; MS/MS, tandem mass spectrometry.

10.1021/bi982304s CCC: $18.00
Published on Web 02/17/1999

mass spectrometry. The fragmentation products of polyglycylated peptides obtained in the mass spectrometer provide information regarding the precise location of modified residues and the extent of modification of each modified residue. The fragmentation process was first characterized with synthetic polyglycylated peptides possessing the same linear sequence as the C-terminal peptides of β-tubulin, and fragmentation rules were established *(11)*. These high-energy collision rules were extended to the low-energy fragmentation obtained from the recent hybrid tandem mass spectrometry technique: nano-electrospray ionization quadrupole orthogonal acceleration time-of-flight (nanoESI Q-TOF) mass spectrometry. This technique allows fragmentation experiments to be conducted on individual peptides from complex mixtures of peptides at the sub-picomole level. This is a major advantage in the analyses of HPLC fractions containing more than one polyglycylated species.

In this work, the strategy described previously *(11)* has been applied to the structural characterization of polyglycylation of β-tubulin from *Paramecium* cytoplasm and axonemes, which involves the determination of both the level of polyglycylation of each isoform and the structure of each level of polyglycylation. The level of polyglycylation of a peptide is defined by the total number of glycine residues posttranslationally added. The structure of a level is given by the location of the modified glutamate residues and by the length of each posttranslationally added polyglycine chain. The research described in this report is separated into four sections. First, we compare the relative abundance of the different isoforms in cytoplasmic and axonemal microtubules by MALDI-TOF MS. Polyglycylation occurs not only in cold-stable axonemal microtubules but also in cold-sensitive intracytoplasmic microtubules *(12, 13)*. Mass spectrometric analysis reveals that cytoplasmic and axonemal tubulins contain the same major level of glycylation with six additional glycine residues. The relative abundance of glycylated isoforms varies inversely with the number of posttranslationally added glycine residues. However, it decreases smoothly and regularly in axonemal microtubules whereas it drops abruptly from six to nine in cytoplasmic microtubules. Second, we optimize the fragmentation with synthetic peptides using both PSD/CID MALDI-TOF MS and nanoESI Q-TOF MS/MS techniques. Third, we apply this strategy to the analysis of the major hexaglycylated isoform. Last, we describe the complete structural study on both cytoplasmic and axonemal pools of C-terminal peptides of β-tubulin from *Paramecium*. The results indicate that polyglycylation occurs on four sites, Glu^{437}, Glu^{438}, Glu^{439}, and Glu^{441} within a single molecule, independent of the total number of additional glycine residues. To each level of polyglycylation correspond clearly several structures (i.e., different levels of modification on each modification site) with at least one major structure. Indeed the degree of structural heterogeneity increases with the degree of polyglycylation. However, the structures established for the common polyglycylation levels of cytoplasmic and axonemal β-tubulin from *Paramecium* are identical.

EXPERIMENTAL PROCEDURES

Materials. Synthetic glycylated peptides were purchased from Neosystem (Strasbourg, France). Their synthesis has been previously described *(11)*. α-Cyano-4-hydroxycinnamic acid was used for all MALDI experiments (Sigma Chemical, St Louis, MO), with nitrocellulose from Millipore Corporation (HAHY, Bedford, MA). Endoproteinase Asp-N sequencing grade was purchased from Boehringer Mannheim GmbH (Mannheim, Germany). Taxol was kindly provided by Dr. D. Guénard (CNRS, Gif/Yvette, France). The different HPLC grade solvents used were TFA, acetone, isopropyl alcohol, acetonitrile, formic acid, and methanol.

Purification of Tubulin from Paramecium tetraurelia Cells (Strain d4−2). (A) Cytoplasmic tubulin. The intracytoplasmic microtubules network is cold-sensitive. Therefore the cytoplasmic extract was recovered by centrifugation, after cold depolymerization of intracytoplasmic microtubules, as described in ref 14. Microtubule proteins were purified by assembly in the presence of taxol, as reported in ref 15.

(B) Axonemal Tubulin. Ciliary axonemes were prepared after selective detachment of cilia from the cell bodies (induced by $MnCl_2$). Tubulin was recovered by sonication of microtubule doublets and purified, as previously described *(16)*.

Preparation of C-Terminal Peptides of Tubulin. Tubulin was digested with endoproteinase Asp-N at an enzyme-to-protein ratio of 1/400 (w/w) at 37 °C for 6 h. The digested protein was separated by anion exchange high-performance liquid chromatography (HPLC) on a diethylaminoethyl column (Waters, DEAE5PW, 7.5 × 75 mm) using a 50 mM to 500 mM NaCl gradient over 1 h in 20 mM Tris-HCl buffer (pH 8). The fraction eluted at the highest salt concentration contained the C-terminal acidic peptides, from both α and β subunits. The α- and β-tubulin peptides were separated by reverse-phase HPLC on a C_{18} column (Vydac, 5 μm, 220 × 2.1 mm) *(4)*. The DEAE HPLC fractions containing the major glycylation levels of C-terminal peptides of axonemal and cytoplasmic β-tubulin were selected, and one-tenth of each was taken to prepare the pooled peptides samples. They were further purified by reverse-phase HPLC. All the samples were finally concentrated to about one-fifth of the volume directly from the elution solvent (acetonitrile/0.1% aqueous TFA 3:7 (v/v)).

Mass Spectrometry (MS). (A) MALDI-TOF. Mass spectra were recorded in MS and CID/PSD MS modes with a Voyager Elite (PerSeptive Biosystems, Inc., Framingham, MA) MALDI-TOF mass spectrometer equipped with a delayed extraction device in optimized ionization conditions with thin-layer preparation of the sample in the presence of α-cyano-4-hydroxycinnamic acid and nitrocellulose, as described in ref 11. A nitrogen laser beam (λ = 337 nm, 3 ns-wide pulse at 20 Hz, laser power set just above the desorption threshold) was focused for desorption on the gold-coated target, and the ions were detected after a total flight length of 3 m. Although fragmentation experiments were run in positive mode, direct MS spectra were acquired in reflectron and negative mode to obtain the best signal-to-noise ratio. Argon was chosen as the collision gas in the CID/PSD mode with a pressure of about 2×10^{-6} mbar. Delayed extraction time was set at a relatively high value between 250 and 350 ns. At least 100 shots were averaged for each mass range acquired before generating the CID/PSD spectrum. External calibration was performed with a mixture of Neurotensin and ACTH (18−39 clip), with monoisotopic masses for $[M + H]^+$ of 1672.92 and 2465.20 Da, respectively.

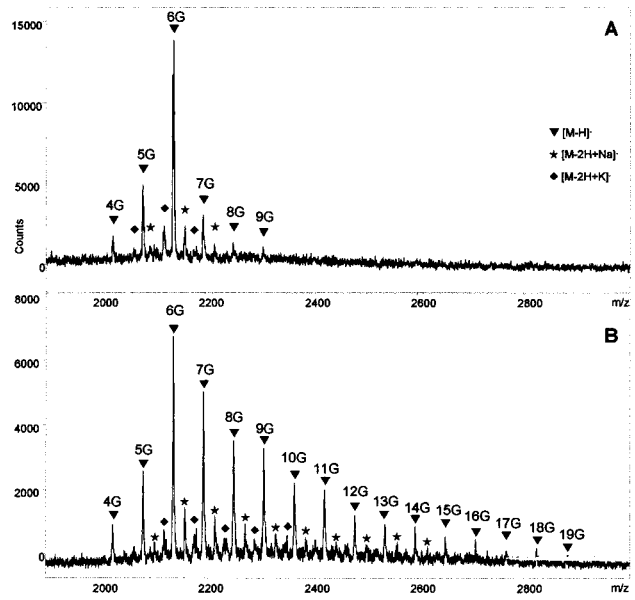

FIGURE 1: MALDI-TOF spectra of major polyglycylated C-terminal peptides of (A) cytoplasmic and (B) axonemal tubulin from *Paramecium*. Glycylation levels are indicated on the top of each peak.

(B) nanoESI Q-TOF. Mass spectra were acquired in MS and MS/MS modes using a Q-TOF (Micromass UK Ltd., Manchester, U.K.) hybrid quadrupole orthogonal acceleration time-of-flight tandem mass spectrometer, as described in ref 17, fitted with a single-shot nanoflow electrospray source in an orthogonal configuration with the Z*SPRAY* (Micromass UK Ltd.) interface. Argon collision gas was used in the MS/MS studies, with the collision energy set at about 30 eV to give optimized fragmentation. When necessary, to improve the signal-to-noise ratio, the concentrated fractions containing the peptides of interest were diluted with twice their volume of methanol/1% aqueous formic acid 1:1 (v/v) prior to introduction into the mass spectrometer, due to the presence of concentrated TFA precluding an efficient ionization process of the peptides.

Edman Degradation. Peptides were sequenced by automated Edman degradation using a Procise model 794 (Perkin Elmer, Applied Biosystems Division, Foster City, CA) pulsed-liquid protein sequencer.

RESULTS

Comparison of the Polyglycylation Profiles in Cytoplasmic and Axonemal Tubulin by MALDI-TOF MS. Polyglycylation has been mostly investigated in very stable microtubules *(2)* and was discovered in axonemal microtubules from *Paramecium (4)*, but TAP 952, an antibody directed against polyglycylation, has also been described to label the cold-sensitive intracytoplasmic microtubules *(12)* and to react with cytoplasmic tubulin *(13)*. After enzymatic digestion of cytoplasmic and axonemal tubulin, C-terminal peptides were isolated by anion exchange HPLC. The most acidic HPLC fractions that were detected by UV absorbance analysis and identified by Edman degradation were pooled with regard to the initial concentration of peptides. MALDI-TOF mass spectra of purified pools of C-terminal peptides of both axonemal and cytoplasmic β-tubulin exhibit two different profiles of polyglycylation. The relative abundance of glycylated isoforms is shown in Figure 1. It differs in cytoplasm (Figure 1A) and in axonemes (Figure 1B). Only the most abundant glycylation levels (total number of glycine residues posttranslationally added on tubulin) are presented with a significant signal-to-noise ratio.

In both cases the major isoform corresponds to the hexaglycylated level β6G,[2] but the relative abundance of higher glycylation levels drops abruptly in the intracytoplasmic microtubules whereas it decreases smoothly in axonemal microtubules. The lower levels, the tetraglycylated β4G and the pentaglycylated β5G levels, are found in the same proportions in axonemal and cytoplasmic preparations. Traces of biglycylated β2G and triglycylated β3G levels can be detected in the cytoplasmic pool *(13)*. Nonglycylated tubulin was never found in these acidic fractions. However, the more glycylated a peptide, the shorter is its associated retention time in anion exchange liquid chromatography *(4)*. The nonglycylated isoform, if any exists, should coelute in the last acidic fractions that were pooled. The results are consistent with immunological analyses: it has been shown that AXO 49 does not decorate intracytoplasmic microtubules but reacts with axonemal microtubules, whereas TAP 952 can decorate both of them *(12)*. Recently, dot-blot studies demonstrated a higher affinity of TAP 952 with peptides possessing monoglycylated residues, and a higher affinity of AXO 49 with peptides possessing lateral polyglycine chains with three or more glycine units *(13)*. All data indicate that the highest levels of polyglycylation are specific to axonemal microtubules. It was therefore interesting to examine if polyglycylation sites were similar in cytoplasmic and axonemal tubulin. It has been shown by Edman degradation that only the four last C-terminal glutamate residues could be glycylated *(4)*. The following sequence indicates in boldface the potential glycylation sites in the C-terminal sequence of β-tubulin, namely Glu^{437}, Glu^{438}, Glu^{439}, and Glu^{441}.

$$^{427}\mathrm{D\ A\ T\ A\ E\ E\ E\ G\ E\ F\ \mathbf{E}^{437}\ \mathbf{E}^{438}\ \mathbf{E}^{439}\ G\ \mathbf{E}^{441}\ Q^{442}} \quad (1)$$

The coexistence of several polyglycylation sites within a single molecule of tubulin would explain that no reactivity of AXO 49 with either in situ microtubules *(12)* or purified tubulin *(13)* was detected in the cytoplasm. It would imply shorter lateral polyglycine chains for a given polyglycylation level. For example the β8G octaglycylated peptide could have four biglycylated glutamate residues. In this case it would not react with AXO 49. The only exception is the very minor β9G peptide: at least one triglycine chain should be linked to one of the four C-terminal glutamate residues. The whole set of data suggests the presence of multiple glycylation sites on *Paramecium* β-tubulin. As shown in the following part, further studies with tandem mass spectrometry confirmed this interpretation.

Mass Spectrometric Study. (A) Optimization of Fragmentation by Mass Spectrometry on Synthetic Peptides. The structural study of polyglycylation can be realized by tandem mass spectrometry. Fragmentation of peptides by mass spectrometry has been well described *(18)*. Acidic peptides are known to give N-terminal and C-terminal fragments

[2] In the following, the C-terminal peptides of β-tubulin will be named βXG, where *X* is the total number of glycine residues not genetically encoded.

Table 1: Specific Internal Fragments[a]

fragment	*m/z*	associated glycylation level
G1	142	monoglycylation
G2	199	biglycylation
G3	256	triglycylation
G4	313	tetraglycylation

[a] The fragments are denoted with G for glycine, followed by the number of included glycine in the fragment. They are observed on CID/PSD MALDI-TOF spectra and sign for the level of glycylation of one single site.

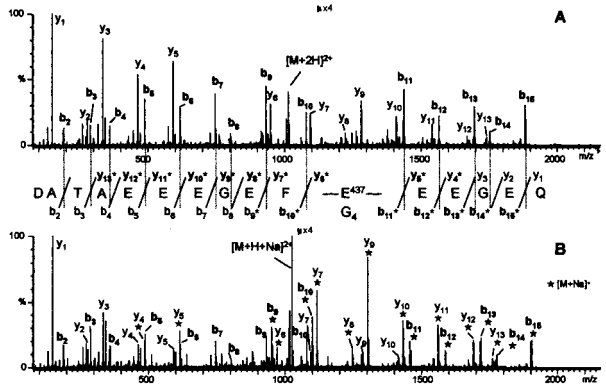

FIGURE 2: Comparison of the nanoESI Q-TOF MS/MS spectra from the synthetic tetraglycylated peptide with A) $[M + 2H]^{2+}$ and B) $[M + H + Na]^{2+}$ as precursors. Peaks marked with stars correspond to sodium adducts on fragments. One picomole was loaded in the nanospray tip.

across the peptide bond with charge retention on acylium (b) or ammonium (y) ion fragments together *(19)*. This powerful tool allows the characterization of polyglycylated sites (location and polyglycylation level of each modified site). The fragmentation process was studied on polyglycylated synthetic peptides, possessing the same linear sequence as the C-terminal peptides of *Paramecium* β-tubulin (see sequence 1). The fragmentation rules are simple: acidic glycylated peptides cleave to form y- and b-type fragments, and the polyglycine side chains do not fragment *(11)*. Losses of neutral water molecules are also observed on most b-fragments. In CID/PSD MALDI-TOF MS mode, we observed certain internal fragments specific to the level of glycylation of each modified site. The masses of the fragments specific to a modified glutamate residue with 1−4 lateral glycine residues are given in Table 1.

These fragments correspond to the cleavage of modified glutamates along with their polyglycine side chain. The nanoESI Q-TOF hybrid tandem MS experiments give the same pattern of fragmentation without the internal fragments. Figure 2 presents the MS/MS spectra obtained with about 1 pmol of a synthetic β4G peptide tetraglycylated on Glu^{437} (see structure in Figure 2).

The complete sequence could be read from in the spectrum (Figure 2A). The mass of the tetraglycylated glutamate has been detected between fragments b_{10} and b_{11} on one hand and between y_6 and y_5 on the other hand. In CID/PSD mode the fragment G4 is also observed (data not shown). The lateral polyglycine chain does not fragment. The ESI Q-TOF spectra appear to be less informative in the low-mass range than CID/PSD mass spectra: none of the internal specific fragments were detected in our fragmentation conditions. But ESI Q-TOF fragmentation analysis has several advantages.

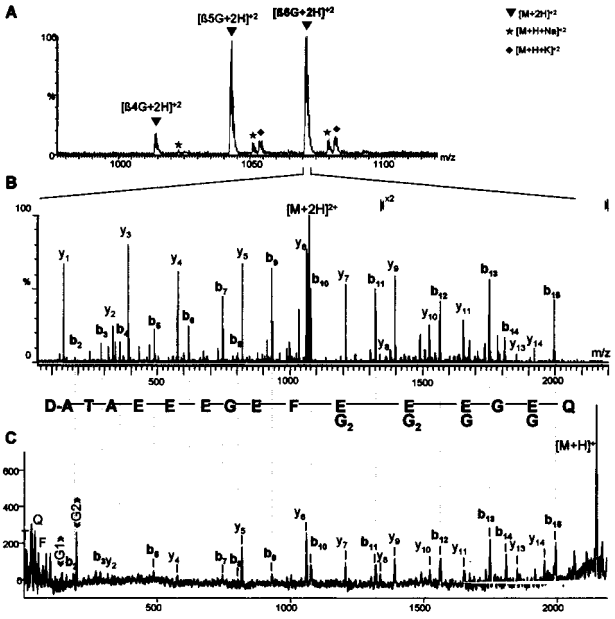

FIGURE 3: Comparison of fragmentation profiles of the C-terminal β6G peptide of cytoplasmic tubulin from *Paramecium*: (A) nanoESI Q-TOF MS spectrum of the HPLC fraction containing the precursor, (B) nanoESI Q-TOF MS/MS spectrum, and (C) CID/PSD MALDI-TOF MS spectrum. The structure of polyglycylation is detailed in parts B and C.

The first advantage is the high specificity of selection of the precursor ion with high selectivity before the collision-activated dissociation (CAD) process. This is of high interest for MS/MS analyses with mixtures of coeluting peptides such as the polyglycylated ones. The selected peptide is the only one that undergoes the fragmentation process with an improved efficiency. Moreover the sensitivity of the two techniques are both in the sub-picomole range. Consequently, MS/MS experiments were performed on minor glycylation levels directly from biological complex mixtures with the Q-TOF configuration. MS/MS spectra often exhibit an enhanced signal-to-noise ratio in comparison with the MS mode. The second advantage is the higher accuracy and resolution of mass measurement of the fragment ions.

The polyglycylated peptides are very difficult to desalt. They interact very strongly with alkaline salts such as sodium or potassium salts. This is thought to be due to their acidic properties. In positive mode and even in negative mode MS experiments, sodium and potassium adducts always give strong signals even after a reverse-phase HPLC purification (see Figure 1). Figure 2 compares the Q-TOF MS/MS spectra acquired on the $[M + 2H]^{+2}$ and the $[M + H + Na]^{+2}$ precursors of the synthetic β4G. The b- and y-type fragments that contain the $^{436}F(E\text{-}G_4)E^{438}$ glycylated internal sequence are observed only with sodium adducts (designated by stars on Figure 2). This suggests that Na^+ cations interact preferentially with the acidic polyglycine carboxylic moieties on the side chain.

(B) Application of Tandem Mass Spectrometry (CID/PSD MALDI-TOF MS and nanoESI Q-TOF MS/MS) to the Characterization of the Major Hexaglycylated Peptide. Figure 3 compares the fragmentation profiles of CID/PSD MALDI-TOF MS and nanoESI Q-TOF MS/MS of the major C-terminal β6G peptide from cytoplasmic β-tubulin. Figure 3A shows the ESI Q-TOF spectrum of the associated reverse-

Table 2: Summary of the Elucidated Structures of Polyglycylated Peptides from *Paramecium* Cytoplasm

glycylation level[a]			
level	*N* calcd	major structure(s)[b]	minor structure(s)[b]
β4G	35	1.1.1.1	1.2.0.1; 0.2.1.1
β5G	56	1.2.1.1 and 2.1.1.1	
β6G	84	2.2.1.1[c]	
β7G	120	(2.3.1.1)	

[a] βXG gives the total number (X) of additional glycines, and N is the total number of hypothetical structures corresponding to each level of glycylation. [b] Structures are given by four numbers equal to the number of glycine residues, respectively linked on Glu[437], Glu[438], Glu[439], and Glu[441]. The cytoplasmic β7G structure is in parentheses because it has been only analyzed by PSD MALDI-TOF MS. [c] See Figure 3.

phase HPLC fraction. It is a mixture of a minor β4G and two major β5G and β6G peptides. Parts B and C of Figure 3 show the MS/MS spectra obtained after selection of the β6G, in ESI Q-TOF and MALDI-TOF, respectively. The ESI spectrum presents a regular and almost complete fragmentation pattern, producing b- and y-type ions, and gives information on the whole sequence. The MALDI spectrum does not exhibit the whole batch of b- and y-type fragments and shows lower signal-to-noise ratio but does, however, allow the complete structural characterization of the polyglycylation. It gives complementary information in the low-mass range, with G1 and G2 fragments signaling the presence of mono- and biglycylated glutamates (see Table 1).

Thus the structure of polyglycylation of this hexaglycylated peptide is

$$^{427}\mathrm{D\,A\,T\,A\,E\,E\,E\,G\,E\,F}\,\underset{G_2}{E}^{437}\,\underset{G_2}{E}^{438}\,\underset{G}{E}^{439}\,\mathrm{G}\,\underset{G}{E}^{441}\,\mathrm{Q}^{442} \quad (2)$$

In the following, this structure will be denoted by β6G-2.2.1.1. It represents[3] a C-terminal hexaglycylated peptide from β-tubulin that bears two additional glycine residues on both Glu[437] and Glu[438] and one additional glycine residue on both Glu[439] and Glu[441]. The results confirm the hypothesis of a polyglycylation occurring at multiple sites. The same approach was consequently generalized for the structural characterization of other glycylation levels from both cytoplasmic and axonemal β-tubulin.

(C) Elucidation of the Structures of Posttranslationally Polyglycylated Peptides from Both Cytoplasm and Axoneme. Cytoplasmic tubulin was primarily studied using CID/PSD MALDI-TOF experiments, and each structure (except β7G) was confirmed by nanoESI Q-TOF MS/MS on less than 500 fmol, as estimated by UV absorbance. Axonemal tubulin was primarily studied using nanoESI Q-TOF MS/MS experiments. Between 500 and 50 fmol of peptides were loaded according to the level of polyglycylation that was analyzed. Structures of β6G and β7G peptides were also determined and confirmed by CID/PSD MALDI-TOF analysis.

Tables 2 and 3 summarize the elucidated structures of polyglycylated C-terminal peptides from cytoplasmic and axonemal β-tubulin. Analyses were run on pooled fractions (as shown in Figure 1) and/or on separate fractions. It was possible to analyze minor structures for peptides that do not copurify with other peptides although they exhibit the same polyglycylation level. For example cytoplasmic β4G-0.2.1.1 is eluted earlier than the major β4G-1.1.1.1 by anion exchange chromatography. In most cases the major structure identified in pooled fractions was similar to the one found in separate fractions.

[3] A C-terminal peptide of β-tubulin with *a*, *b*, *c*, and *d* additional glycine residue(s) on, respectively, Glu[437], Glu[438], Glu[439], and Glu[441] will be denoted βXG-*a.b.c.d* (where $X = a + b + c + d$).

Table 3: Summary of the Elucidated Structures of Polyglycylated Peptides from *Paramecium* Axonemes

glycylation level[a]			
level	*N* calcd	major structure(s)[b]	minor structure(s)[b]
β4G	35	1.1.1.1	4.0.0.0
β5G	56	1.2.1.1 and 2.1.1.1[c]	
β6G	84	2.2.1.1	2.2.0.2
β7G	120	2.3.1.1	2.2.0.3
β8G	165	2.2.2.2	2.2.1.3, 3.1.2.2, 2.3.1.2, 3.2.0.3, 3.2.1.2
β9G	220	2.2.2.3	2.3.1.3, 3.1.2.3, 2.3.2.2, 2.3.2.3
β10G	286	2.3.2.3	3.2.2.3, 4.1.2.3, 2.2.4.2, 2.2.3.3, 2.3.3.2, 2.4.1.3
β11G	364	2.3.3.3 and 2.4.2.3	
β12G	455	2.?.?0.3[d]	(2 to 5).?.?.(3 to 5)
β13G	560	2.5.3.3, 2.6.2.3, 3.4.3.3, 3.5.2.3	

[a] βXG gives the total number (X) of additional glycines, and N is the total number of hypothetical structures corresponding to each level of glycylation. [b] Structures are given by four numbers equal to the number of glycine residues, respectively linked on Glu[437], Glu[438], Glu[439], and Glu[441]. The cytoplasmic β7G structure is in parentheses because it has been only analyzed by PSD MALDI-TOF MS. [c] See Figure 4. [d] See Figure 5.

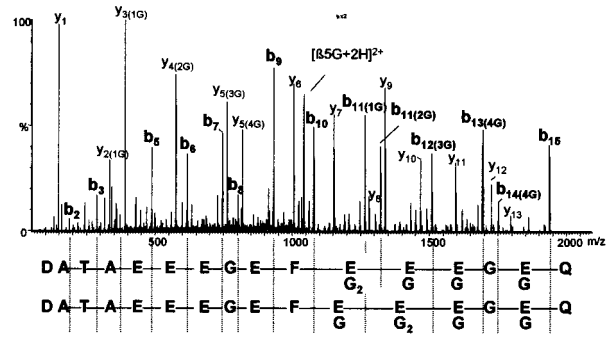

FIGURE 4: nanoESI Q-TOF MS/MS spectrum of the C-terminal β5G peptide of axonemal tubulin from *Paramecium*.

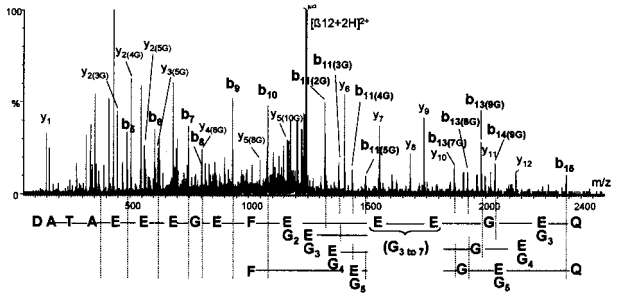

FIGURE 5: nanoESI Q-TOF MS/MS spectrum of the C-terminal β12G peptide of axonemal tubulin from *Paramecium*.

Figures 4 and 5 present two examples of MS/MS spectra of axonemal C-terminal peptides from β-tubulin. The first was obtained from a quite homogeneous level (β5G, Figure 4) in terms of the number of elucidated structures and the second from a much more heterogeneous one (β12G, Figure 5).

The β5G level in both axonemal and cytoplasmic tubulin is constituted of two major structures that coexist in the same purified fractions. Both techniques gave consistent and unambiguous results (Figure 4 presents, for example, the nanoESI Q-TOF MS/MS analysis).

The coexistence of the two structures is demonstrated by the presence in the spectrum of two peaks: $b_{11(1G)}$ and $b_{11(2G)}$, at mass-to-charge ratios (*m*/*z*) of 1265.2 and 1322.1, respectively. They correspond to the N-terminal fragment from Asp^{427} to Glu^{437} with one and two glycine residue(s) on the last Glu^{437}, respectively. The spectrum exhibits two peaks, $y_{5(4G)}$ and $y_{5(3G)}$, at *m*/*z* ratios 819.2 and 762.2, respectively. They correspond to the C-terminal fragment from Glu^{438} to Gln^{442} with four and three glycine residue(s) on the last three glutamate residues, respectively. Therefore, it confirms that the residue Glu^{437} can bear, respectively, one and two glycine residue(s).

The MS/MS spectrum of β12G is much more complex (see Figure 5). It accounts for the structural heterogeneity of this level. It is worth noticing the presence of four peaks, $b_{11(2G)}$, $b_{11(3G)}$, $b_{11(4G)}$, and $b_{11(5G)}$, at *m*/*z* ratios 1322.5 and 1379.5, 1436.6, and 1493.6, respectively. They correspond to the N-terminal fragment from Asp^{427} to Glu^{437} with two, three, four, and five glycine residue(s) on the last Glu^{437}, respectively. Another interesting set of peaks at *m*/*z* ratios 1865.6, 1922.8, 1979.6, and 2036.9 corresponds to either $b_{13(7G)}$, $b_{13(8G)}$, $b_{13(9G)}$, and $b_{13(10G)}$ or $b_{14(6G)}$, $b_{14(7G)}$, $b_{14(8G)}$, and $b_{14(9G)}$. The b_{13} and b_{14} fragments correspond to the N-terminal fragments from Asp^{427} to Glu^{439} and Gly^{440}, respectively. Thus, they bear the same number of additional glycine residues. Even though b_{14} is weak, it was always seen by Q-TOF MS/MS. Therefore, the final interpretation associates *m*/*z* 1865.6 to $b_{13(7G)}$, *m*/*z* 1922.8 to both $b_{13(8G)}$ and $b_{14(7G)}$, *m*/*z* 1979.6 to both $b_{13(9G)}$ and $b_{14(8G)}$, and *m*/*z* 2036.9 to $b_{14(9G)}$. It ensues that three to five glycine residues can be added on the Glu^{441} residue. It was not possible to discriminate between the different possible distributions of other residual glycine residues on Glu^{438} and Glu^{439}. The analysis shows that the four C-terminal glutamate sites of the molecule are involved in the posttranslational polyglycylation.

Not all of the structures are listed in the tables. Only the major ones are presented. It is remarkable that β6G (Figure 3) has only one major structure and β5G (Figure 4) two equivalent major ones, with no minor structures observed both on cytoplasmic and axonemal preparations. On the contrary, the higher levels are more heterogeneous, with heterogeneity increasing with the number of added glycine residues. Most of the time, this precludes a complete interpretation of MS/MS spectra (Figure 5).

DISCUSSION

Polyglycylated Levels Exhibit Relatively Homogeneous Structures. In the present study, β-tubulins bearing from four to nine posttranslationally added glycine residues are observed in both cytoplasm and axonemes. However, the amounts of levels of polyglycylation higher than the major hexaglycylated level drop abruptly in cytoplasmic tubulin, whereas they decrease regularly and smoothly with the number of added glycine residues in axonemal tubulin (Figure 1). Mass spectrometry is well adapted for the structural characterization of proteins available in very low amounts *(11)*. All the spectra were obtained at the subpicomole range (at the very most, half a picomole has been used for the structural characterization of the major hexaglycylated peptide).

Tables 2 and 3 provide structures of polyglycylated C-terminal peptides of cytoplasmic (Table 2) and axonemal (Table 3) β-tubulin. The major structures for each glycylation level are common to cytoplasmic and axonemal preparations. In both of them, the glycylation occurs on the last four C-terminal glutamate residues of the encoded sequence. No preferential modification site could be identified. As recently reported, polyglutamylation, the other tubulin specific polymodification, can also occur on multiple sites *(20, 21)*. Moreover, the structural heterogeneity increases with the number of posttranslationally added glycine units.

The number of structures has to be compared to the calculated number *N* of the potential theoretical structures given in Tables 2 and 3. Even if the results show a structural heterogeneity within some levels of polyglycylation, it is not comparable to the theoretical number of available structures. For example, among the 56 calculated structures of the pentaglycylated peptide, only two are confirmed by mass spectrometry.

Two features are striking. First, the common polyglycylation levels in axonemal and cytoplasmic β-tubulin present the same major structures. Second, it is always possible to go from one glycylation level to the next one by simply adding/removing one glycine residue at one site. Consider, for example, the following sequence of major structures: β4G-1.1.1.1, β5G-(1.2.1.1 or 2.1.1.1), β6G-2.2.1.1, β7G-2.2.1.2, β8G-2.2.2.2, β9G-2.2.2.3, β10G-2.3.2.3, ...

Glycine residues are evenly distributed among the last four glutamate residues Glu^{437}, Glu^{438}, Glu^{439}, and Glu^{441}. This explains the different immunoreactivities of AXO 49 and TAP 952 with isolated cytoplasmic and axonemal tubulin *(13)* and with the corresponding microtubular networks *(12)*. AXO 49 specifically recognizes polyglycine chains possessing at least three glycine units *(13)*. The major cytoplasmic structures do not present any triglycylated glutamate (Table 2). So AXO 49 should specifically label axonemal microtubules. This specificity was experimentally confirmed: AXO 49 reacts strongly with *Paramecium* cilia but does not label the intracytoplasmic network. On the opposite, TAP 952 was shown to strongly react with a synthetic β4G-1.1.1.1 *(13)*. The latter was found in both cytoplasmic and axonemal microtubules (Tables 2 and 3). Experimentally TAP 952 reacts strongly with the intracytoplasmic network and with ciliary axonemes. Mass spectrometry appears to be a useful tool for the characterization of antibody epitopes.

Polyglycylation Involves at Least Four Different Enzymatic Activities. At present time, none of the enzymes involved in the posttranslational polyglycylation have been characterized. Our structural data suggest that at least four different enzymatic activities could be involved in the polyglycylation process. The first two would involve a glycine transferase activity (of type EC 2.3.2.X following the IUPAC enzyme classification). The first activity would be a glycine γ-glutamyltransferase activity. It recognizes the γ-carboxylic moiety of the four last glutamate residues and links the first glycine residue. The second activity would be a glycine glycyltransferase. It links the next glycine residues

during the elongation step of polyglycine chains on tubulin. The fact that nonmodified β-tubulin has not been detected and that the major β4G peptide is β4G-1.1.1.1 in both cytoplasmic and axonemal β-tubulin could indicate that all the modification sites of β-tubulin may be glycylated by the glycine γ-glutamyltransferase before microtubule assembly and before the beginning of the polyglycine elongation step. The action of glycine glycyltransferase is not limited to the synthesis of one major structure but leads to many different "byproducts", as demonstrated by the existence and the heterogeneity of high levels of polyglycylation in axonemal tubulin. Two different peptidases (both of type EC 3.4.X) would be involved in counteracting the glycine transferase activity: a glycyl glycine carboxypeptidase, cleaving the C-terminal glycyl−glycine bond, and a γ-glutamylhydrolase activity, cleaving the γ-glutamyl bond to release an unsubstituted C-terminal glutamate residue. The glycyl glycine carboxypeptidase may regulate the effects of the glycine glycyltransferase to maintain the major β6G-2.2.1.1 structure by removing superfluous glycine residues in both axonemal and cytoplasmic tubulin. Indeed a glycyl glycine carboxypeptidase activity has been detected in the cytoplasm of *Paramecium (13)*. The glycine glycyltransferase may act more efficiently on the polymerized tubulin of stable axonemal microtubules than on the cytoplasmic ones. This could explain the drop of relative amounts of isoforms bearing more than six additional glycine residues in the cytoplasmic pool. The γ-glutamylhydrolase activity—combined (or not) with the glycine carboxypeptidase—may allow the regeneration of nonmodified glutamate γ-carboxyl moieties by removing all the posttranslationally added glycine residues. This hypothesis would explain the presence of the minor isoforms such as β4G-4.0.0.0. In general, all the observed structures could be explained by a balance of these four enzymatic activities. Regnard et al. *(22)* have recently described the first purification of an enzyme responsible for tubulin polyglutamylation. Their results are also in favor of a sequential mechanism for the glutamate addition, which involves several different enzymes to explain the diversity of tubulin polyglutamylation in cells.

Our structural study suggests the formation of a negatively charged bulky C-terminal domain. It differs from the structure of one long polyglycine side chain linked to one glutamate residue that has been inferred *(1)*. The distribution of glycine residues on the four C-terminal glutamate residues prevents sterical hindrance of nonmodified glutamate γ-carboxyl moieties as would be the case in a mono-site polyglycylation. Intramolecular hydrogen bonding involving large ring interactions has been described in triglycine chains *(23)*. The polyglycine chains could also interact with each other. Hydrogen bonding between the four glycine side chains and neighboring glutamate residues would impose considerable stability on the microtubule lattice. This C-terminal domain is known to be located on the outer surface of microtubular structures and is likely to form a moving and variable domain. No three-dimensional structural data are available on this domain *(24)*. Thus, the whole external surface of the microtubule is surrounded by negatively charged mobile acidic groups that may affect interactions between microtubules and microtubule-associated proteins (MAPs). The β6G-2.2.1.1 structure should result in a particular three-dimensional configuration at the end of the C-terminal domain. This major structure might play a functional role in mediating the interactions between microtubules and MAPs, cationic species, and/or membrane proteins.

ACKNOWLEDGMENT

This work was supported by the Association pour la Recherche contre le Cancer (ARC, France). It forms a portion of the doctoral thesis of J. Vinh, who received predoctoral fellowships from the Centre National de la Recherche Scientifique (CNRS, France) and Synthélabo Recherche (France). We thank J.-P. Le Caer for his thoughtful and judicious advice and Jennifer Brunton for correction of the manuscript.

REFERENCES

1. Luduena, R. F. (1998) *Int. Rev. Cytol. 178*, 207−75.
2. MacRae, T. H. (1997) *Eur. J. Biochem. 244*, 265−78.
3. Mandelkow, E., and Mandelkow, E. M. (1995) *Curr. Opin. Cell Biol. 7*, 72−81.
4. Redeker, V., Levilliers, N., Schmitter, J. M., Le Caer, J.-P., Rossier, J., Adoutte, A., and Bré, M.-H. (1994) *Science 266*, 1688−1691.
5. Rüdiger, M., Plessmann, U., Rüdiger, A. H., and Weber, K. (1995) *FEBS Lett. 364*, 147−51.
6. Mary, J., Redeker, V., Le Caer, J.-P., Rossier, J., and Schmitter, J. M. (1996) *J. Biol. Chem. 271*, 9928−9933.
7. Weber, K., Schneider, A., Müller, N., and Plessmann, U. (1996) *FEBS Lett. 393*, 27−30.
8. Bressac, C., Bré, M.-H., Darmanaden-Delorme, J., Laurent, M., Levilliers, N., and Fleury, A. (1995) *Eur. J. Cell Biol. 67*, 346−355.
9. Levilliers, N., Fleury, A., and Hill, A. M. (1995) *J. Cell Sci. 108*, 3013−28.
10. Bré, M.-H., Redeker, V., Quibell, M., Darmanaden-Delorme, J., Bressac, C., Cosson, J., Huitorel, P., Schmitter, J. M., Rossier, J., Johnson, T., Adoutte, A., and Levilliers, N. (1996) *J. Cell Sci. 109*, 727−738.
11. Vinh, J., Loyaux, D., Redeker, V., and Rossier, J. (1997) *Anal. Chem. 69*, 3979−85.
12. Fleury, A., Callen, A.-M., Bré, M.-H., Iftode, F., Jeanmaire-Wolf, R., Levilliers, N., and Clérot, J.-C. (1995) *Protoplasma 189*, 37−60.
13. Bré, M. H., Redeker, V., Vinh, J., Rossier, J., and Levilliers, N. (1998) *Mol. Biol. Cell 9*, 2655−2665.
14. Bré, M.-H., de Néchaud, B., Wolff, A., and Fleury, A. (1994) *Cell Motil. Cytoskeleton 27*, 337−349.
15. Vallee, R. B., and Collins, C. A. (1986) *Methods Enzymol. 134*, 116−127.
16. Geuens, G., Hill, A. M., Levilliers, N., Adoutte, A., and De Brabander, M. (1989) *J. Cell Biol. 108*, 939−953.
17. Morris, H. R., Paxton, T., Dell, A., Langhorne, J., Berg, M., Bordoli, R. S., Hoyes, J., and Bateman, R. H. (1996) *Rapid Commun. Mass Spectrom. 10*, 889−896.
18. Johnson, R. S., Martin, S. A., and Biemann, K. (1988) *Int. J. Mass Spectrom. Ion Processes 86*, 137.
19. Biemann, K. (1990) *Methods Enzymol. 193*, 886−887.
20. Redeker, V., Rossier, J., and Frankfurter, T. (1998) *Biochemistry 37*, 14838−14844.
21. Schneider, A., Plessmann, U., Felleisen, R., and Weber, K. (1998) *FEBS Lett. 429*, 399−402.
22. Regnard, C., Audebert, S., Desbruyeres, Denoulet, P., and Eddé, B. (1998) *Biochemistry 37*, 8395−404.
23. Carr, S. A., and Cassady, C. J. (1996) *J. Am. Soc. Mass Spectrom. 7*, 1203−1210.
24. Nogales, E., Wolf, S. G., and Downing, K. H. (1998) *Nature 391*, 199−203.

BI982304S